Analysis of the accuracy, stiffness and stability of shell structures of mirror antennas using computer modelling

Andrii Sverstiuk[1,2,*,†], Taras Dubynyak[2,†], Mykola Stashkiv[2,†], Volodymyr Nevozhai[2,†] and Mykola Poshyvak[2,†]

[1] *I. Horbachevsky Ternopil National Medical University, Maidan Voli, 1, Ternopil, 46002, Ukraine*
[2] *Ternopil National Ivan Puluj Technical University, Rus'ka str. 56, Ternopil, 46001, Ukraine*

Abstract

During the study, the process of shaping reflective shells and determining the positions of grid elements post-deformation was explored. The mesh nodes were fixed using an electric arc spraying method. The outcome of the research was the successful formation of the antenna array's shell using the electric arc spraying technique alongside the application of a composite material. The interaction between axisymmetric and non-axisymmetric shells, as well as bending vibration modes, which can lead to unstable motion patterns, was examined in detail. The construction of the mirror, consisting of spherical and cylindrical shells connected via a ring, was outlined. The influence of the shell's behavior during the ring's motion, caused by pulse pressure, was taken into account by incorporating contact forces of interaction, which were derived by solving relevant mating contact problems. The stiffness and strength characteristics of both solid and reinforced antenna structures were evaluated and visually depicted, and their stress and deformation states were calculated under external forces such as wind pressure and gravity.

Keywords

electric arc spraying, mesh, reinforced composite material, punch, offset antenna.

1. Introduction

Statement of the problem. The development of antenna systems and the creation of reflective surfaces rely on innovative technological and design approaches. Successful implementation of these innovations requires the necessary scientific and technical backing, which is achievable through close collaboration between industry and scientific expertise. The method of producing mesh material shells can be utilized for manufacturing both axisymmetric and non-axisymmetric reflectors, as well as individual components of mirror antennas [1].

Analysis of known research results. The article deals with the methods of manufacturing antenna systems and reflective surfaces based on new technological and design ideas. The

[1] ITTAP'2024: 4th International Workshop on Information Technologies: Theoretical and Applied Problems, October 23-25, 2024, Ternopil, Ukraine, Opole, Poland
* Corresponding author.
† These authors contributed equally.
sverstyuk@tdmu.edu.ua (A. Sverstiuk);d_taras@ukr.net (T. Dubyniak); stashkiv@tntu.edu.ua (M. Stashkiv); v.nevo1971@gmail.com (V. Nevozhai); claruspuer01@gmail.com (M. Poshyvak)
0000-0001-8644-0776 (A. Sverstiuk);0000-0003-1529-6951 (T. Dubyniak); 0000-0002-7325-8016 (M. Stashkiv);0009-0004-2003-4280 (V. Nevozhai); 0009-0009-9655-4123 (M. Poshyvak)

process of shell formation from mesh material is investigated. The complexity of describing the deformation process lies in the fact that the mesh behaves qualitatively differently when deformed than a sheet of solid material. This is due to its structure, in particular, the ability to rotate mutually perpendicular mesh wires relative to each other at the nodes. Both Ukrainian and international scientists have contributed to the design, development, and production of the mesh, as highlighted in [2, 3]. In Ukraine, the manufacturing was carried out by the Saturn and Promin enterprises, in addition to contributions from renowned international firms such as Siemen sand Andrew.

This paper addresses the issue of local stability under load conditions. It is crucial to investigate the related challenges that arise due to edge dynamic loads generated by the vibrations of the antenna mirror, which are transmitted from the base.

The study explores the dynamic stability of a mirror structured as a spherical segment bonded to a ring. To maintain consistency, it is assumed that a cylindrical shell of finite length is attached to this ring (viewing the antenna mirror as a single spherical shell is regarded as a specific case). The addition of a cylindrical shell is a design choice intended to protect the antenna from external environmental factors, including incoming airflow. After a pulse is applied, the motion consists of both axisymmetric and bending vibrations, which stem from unavoidable inconsistencies within the pulse's distribution.

Purpose of the study. The primary design and technological concepts incorporated into antenna systems include:

optimization of structures according to the criteria of stiffness, accuracy and weight;

use without slipway assembly and on-site adjustment of antennas;

use of vector diffraction methods in optimizing the electrodynamic characteristics of an antenna system at the design stage [4].

The antenna positioning control system, control of its movement speed, diagnostics of its condition during operation, self-testing, is based on digital information processing [5].

The interplay between axisymmetric and non-axisymmetric shells, along with various bending oscillation modes, has been explored, focusing on the development of unstable motion patterns. The construction of the mirror involves spherical and cylindrical shells joined by a ring. The shell acts as an elastic foundation for the ring, constraining its movement. When analyzing the ring's motion under the influence of pulse pressure, the shell's effect is accounted for by incorporating contact interaction forces, which are calculated by solving the relevant contact coupling problems.

2. Principles of satellite communication antennas operation

Choosing satellite TV means having many channels in excellent resolution. Unlike cable TV, satellite TV is available everywhere. All you need is a satellite dish and a decoder. Installation and setup of the equipment is affordable. A satellite TV dish is used to receive a TV signal from a space satellite. The parameters of the dish itself and its converter largely determine the image and sound quality that the satellite decoder will produce on the TV screen. Let's look at the principle of their operation [6].

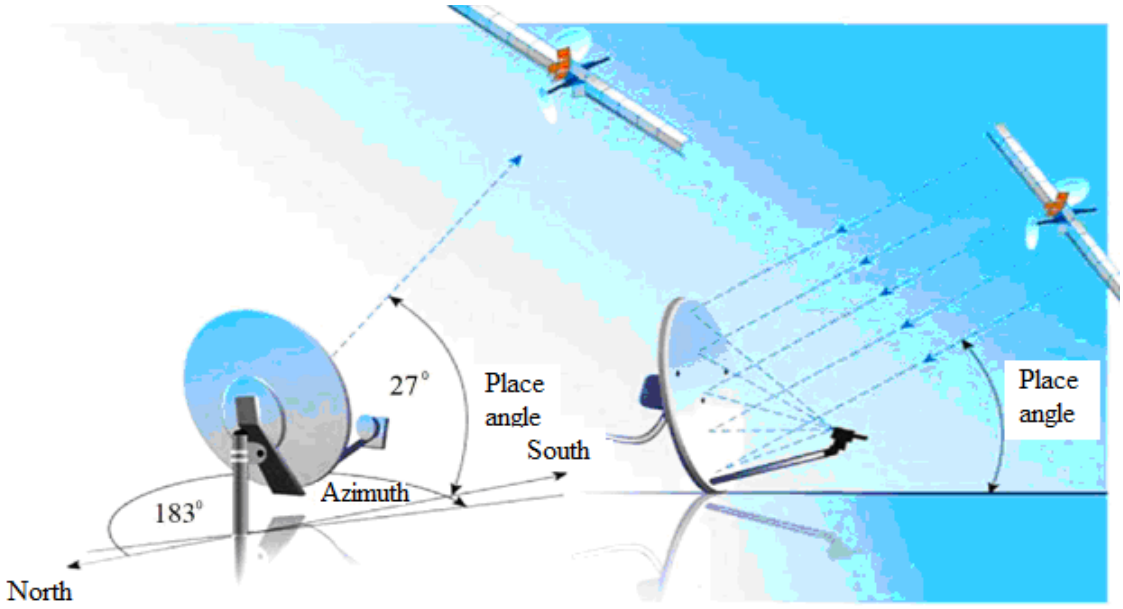

Figure 1: Operation of the satellite dish.

The level of the signal received from the earth satellite is very low compared to its original level: the attenuation is about 200 dB. This is understandable: the distance between the earth and the satellite is about 36000 km. The only way to get a signal of such strength to watch programs is to concentrate it as much as possible. This is the function of the satellite wave receiver, which is a curved surface called a dish. The waves sent by the satellite to the earth are reflected by the inner surface of the antenna, obeying the laws of optics, and are concentrated at a point called the focus. At this point is the receiving head 18 of the converter, a device for converting high-frequency vibrations into a cable signal [7]. Since the discovery of satellite communications, many types of wave receivers have been created to receive and transmit signals. Each type has found its ground application depending on the purpose of the satellite communications system: mobile communications; satellite telephony and radio broadcasting; navigation via orbital communications; the Internet; meteorology; communication with spacecraft; television.

Figure 2: Offset satellite antenna.

Figure 3: Direct-focus satellite dish.

An offset satellite TV antenna resembles a bowl and has an ellipsoidal shape. The signals from the satellites reflected from the working mirror are concentrated above the geometric center of the shape, and its lower focus. A dish with a lower focus does not require a large elevation angle. Such a mirror design in offset satellite dishes allows for more stable reception, since the signal converter does not cast a shadow on the surface of the dish and does not cause noise. Direct-focus satellite dish.

This type of wave receiver has a working mirror surface in the form of a flattened paraboloid. This symmetrical geometry of the reflector allows for good capture of radio waves arriving on its surface and their maximum redirection to the transducer.

The reflector is positioned on the holder's cantilevers, situated directly above the central point of the dish [8].

Analysis of types of mirror antennas

Mirror antennas:

Parabolic and parabolic.

Axisymmetric designs include one-mirror and two-mirror configurations (following the Cassegrain or Gregory arrangement), as well as offset antennas. These designs offer high directivity, broad bandwidth, and a relatively straightforward construction. However, at higher frequencies, precision in manufacturing becomes critical, because even small deviations can affect performance (order deviation).

Circular polarization can be achieved either through the design of the irradiator or by adding extra components, though the latter may increase complexity and weight. Based on the analysis, the most appropriate antenna type for CIC is a single-mirror parabolic antenna, which we will examine more closely. It is widely acknowledged that mirrored parabolic antennas come in both prime focus (direct-focus) and offset configurations.

Direct-focus antennas are also referred to as axisymmetric antennas. Their mirror is shaped like a paraboloid of rotation, giving the antenna a round form where the geometric axis alignswith the electrical axis. Typically, the converter is positioned along this same axis and is mounted to the edges of the reflector using three or four support racks.

An offset antenna is essentially a section taken from a paraboloid. Typically, this section is created by the intersection of a paraboloid and a cylinder, with their axes oriented parallel to each other. As a result, the mirror of the offset antenna takes on an elliptical shape, and the electric axis of the antenna forms an angle with its geometric axis. Generally, the electric axis is positioned 20 to 30 degrees above the geometric axis [9].

The structural design of both direct-focus and offset antennas is illustrated in Figure 4.Both antennas have advantages and disadvantages.

For example, if we consider a direct-focus antenna, it makes more efficient use of the mirror area (Figure 4). An offset antenna provides the same effective area as a direct-focus antenna but with a diameter corresponding to the size of the offset antenna along its minor axis.

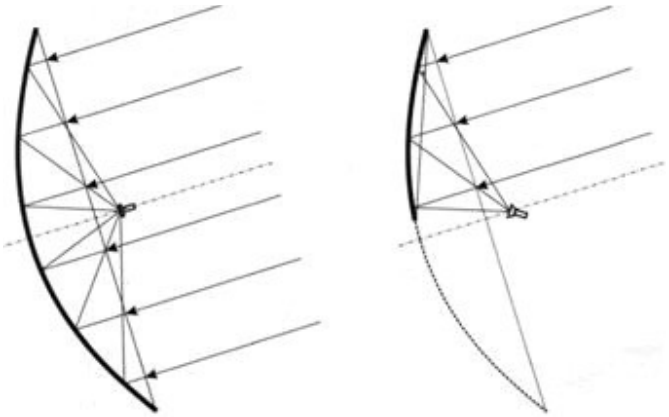

a) b)

Figure 4: Geometry of direct-focus (a) and offset antennas (b).

In other words, to calculate the effective area of an offset antenna, its physical area should be multiplied by the cosine of the angle between the electrical and geometric axes. In typical designs, 86-90% of the physical area is efficiently utilized. In comparison, a direct-focus antenna has part of its surface obstructed by the converter and the mounting components, an issue not present in offset antennas. Consequently, smaller antennas—those up to 1.5 meters in diameter, where the converter may obscure more than 10% of the area—are usually designed as offset antennas, while larger antennas tend to be direct-focus [10].

Given that the antenna will have a diameter exceeding 1.5 meters to achieve the necessary gain, and the converter will cover less than 10% of the antenna's surface area, we have opted for a single-mirror parabolic antenna type with a direct-feed design.

Properties and Applications of a Direct-Focus Single-Mirror Parabolic Antenna: Parabolic antennas are widely employed in space communications and radio relay systems. Their ability to focus signals effectively makes them suitable for long-distance, high-frequency applications. Notably, in 1888, the renowned German physicist Heinrich Hertz first utilized a parabolic cylinder as a receiver in his groundbreaking experiments in microwave optics.

Mirrored parabolic antennas are the most prevalent type of directional antennas used in the centimeter, decimeter, and partial meter wavelength ranges. They are favored for their simplicity, ease of construction, ability to generate a wide variety of radiation patterns, highefficiency, low noise levels, and broad frequency coverage. Certain designs can achieve rapid beam steering across a wide angular sector.

These antennas are also extensively used in space communications and radio-relay systems. Through the use of mirrored parabolic antennas, massive antenna systems are now being developed, with effective surface areas reaching thousands of square meters.

The essential components of a parabolic antenna include a metal reflector (mirror) shaped according to a parabolic curve, an irradiator mounted at the focus of the surface, and a feeder, as shown in Figure 5.

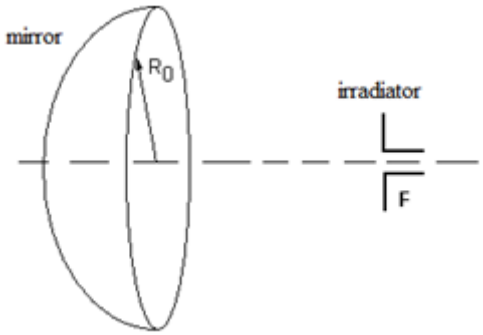

Figure 5: Basic elements of a parabolic antenna.

A weakly directed irradiator, such as a pole, positioned at the focal point of the rotational paraboloid, generates the shape and transforms the spherical wave front into a flat one. The radiator of the antenna is designed to ensure that nearly all of the emitted energy is aimed directly at the reflector [11].

As the electromagnetic waves hit the reflector, they induce high-frequency currents on its surface, which create their own electromagnetic fields. Parabolic antennas capitalize on the optical properties of radio waves. The distinct geometry of the parabola ensures that waves originating from the focal point are reflected such that they travel parallel to the axis of the parabola (as shown in Figure 6). This setup ensures that the path length from the focal point, to the parabola, and then to the aperture line between the parabola's edges, remains uniform regardless of the angle. Consequently, an in-phase surface is formed at the parabolic antenna's aperture, focusing the antenna's radiation into a highly directional beam.

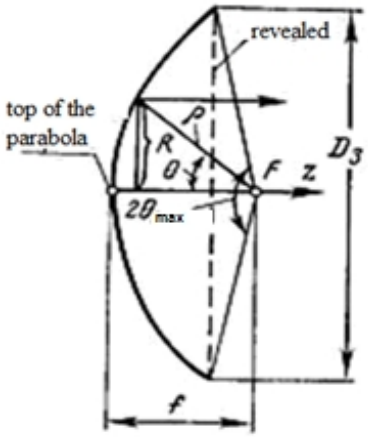

Figure 6: Geometric properties of a parabola.

In the Cartesian coordinate system, a paraboloid of revolution, where the origin is aligned with the vertex of the paraboloid, is mathematically described by the equation:

$$x^2 + y^2 = 4\,fz \tag{1}$$

The rupture diameter of the paraboloid D_3 and its focal length f are related by the ratio:

$$D_3 = 4f \cdot tg(2 \cdot \theta_{\max}) \quad (2)$$

where $2 \cdot \theta_{\max}$ is the opening angle of the paraboloid.

A direct-focus (axisymmetric) antenna features an aperture shaped like a paraboloid of revolution. The mirror of this antenna is parabolic, and both its geometric and electrical axes are aligned. The converter, responsible for signal processing, is positioned along this axis and is typically mounted to the reflector through three or four support arms. The antenna's diameter plays a key role in determining its signal gain and the reliability of satellite signal reception. For geostationary satellites, the diameters of such antennas usually span from 0.55 meters to 3.7 meters. These antennas are commonly employed to receive signals in both the C-band and Ku-band frequencies. Parabolic antennas also function in satellite signal transmission. They are equipped with low-noise amplifiers (LNAs) and converters connected to the irradiators, which help amplify high-frequency signals at the irradiator stage and convert them into intermediate frequency signals. These intermediate signals are then relayed via cables to converters for further amplification and processing [12].

The offset antenna is the most widely used type for individual satellite television reception, although various other designs are also in use for terrestrial satellite dishes. It is essentially an asymmetric section taken from a paraboloid of revolution, with the irradiator positioned at the paraboloid's focal point. Typically, this section is formed by the intersection of a paraboloid and a cylinder with parallel axes. As a result, the mirror of the offset antenna has an elliptical shape, and its electrical axis is positioned at an angle to its geometric axis. Generally, the electrical axisis elevated 20-30 degrees above the geometric axis. This design prevents the irradiator and its mounting elements from casting shadows on the functional area of the antenna, thus improving its efficiency compared to an axisymmetric antenna with the same mirror surface.

Moreover, the irradiator is positioned below the antenna's center of gravity, which enhances the structure's stability in windy conditions. The mirror of the offset antenna is typically mounted in a near-vertical position, with its angle of inclination slightly varying based on geographical latitude. This vertical alignment helps avoid the accumulation of precipitation, which can otherwise degrade signal reception. Instead of being perfectly circular, the antenna’s shape is an ellipse, elongated vertically. When comparing the dimensions of an offset antenna with a direct-focus antenna, the offset design is approximately 10% taller vertically, assuming the horizontal size is kept identical.

Offset antennas are commonly employed to receive signals in the C- and Ku-bands, supporting both linear and circular polarization. Additionally, they are capable of receiving signals in the Ka-band and can handle combined signal types as well.

Advantages and disadvantages.

Both direct-focus and offset antennas come with distinct advantages and disadvantages. A direct-focus antenna typically makes more efficient use of its mirror surface. In contrast, an offset antenna has the same effective area as a direct-focus antenna, but with a diameter defined by the minor axis of the offset mirror. To calculate the effective area of an offset antenna, its physical area is multiplied by the cosine of the angle between the electrical and geometric axes. In general, offset antennas utilize about 86-90% of their physical surface area. A direct-focus antenna, however, experiences some loss of surface area due to obstruction from the converter and its support structures, a problem not present in offset designs. As a result, antennas with a

diameter up to 1.5 meters—where the converter can block more than 10% of the surface—are usually made as offset designs, while larger antennas tend to be direct-focus.

Another consideration is orientation. A direct-focus antenna is set at a fixed positive angle—essentially forming a "bowl"—which can collect precipitation such as rain, snow, or ice. Offset antennas, on the other hand, particularly in northern latitudes, are mounted almost vertically, or even tilted slightly downward, avoiding this issue altogether. However, with direct-focus antennas, the converter faces downward, allowing for the safe use of an uncovered or partially covered irradiator, as water and snow are less likely to enter. In contrast, an offset antenna has its converter facing upward, so it must be properly sealed to prevent water ingress, which could damage the electronic components of the converter.

3. Dynamic local stability of mirror antenna elements

In [13], a comparable method was applied to investigate the dynamic stability of a cylindrical shell incorporating an elastic aggregate. For a cylindrical shell, we apply the equation of the principal stress state and consider various boundary conditions. The equation of motion is written in the form

$$u^{Iv} + \left(1 + s^2\right)u^{II} + s^2\left(1 + u\right) + pR^3\left(EI\right)^{-1} + u = 0 \tag{3}$$

Roman numerals and dots indicate the differentiation in φ dimensionless time $\tau; u = \omega / R; s^2 = NR^2 / EI; \tau = cat / R, c^2 = E / \rho; a^2 = I / R^2 F;$

where ρ is the density of the material; N is the circumferential force in the ring; p *is* the reaction to the ring from the shell; t is time.

If we consider the ring as a strip of thickness and unit width, i.e., as part of the shell, then $I = h^3 / 12, a^2 = h^2 / 12R^2$.

The solution to equation (3) is given by

$$\begin{aligned} &u\left(\varphi,\tau\right) = u_0 + \sum_2^\infty u_n\left(\varphi,\tau\right), \\ &u_n = b_n\left(\tau\right)\cos n\varphi + d_n\left(\tau\right)\sin n\varphi \end{aligned} \tag{4}$$

The term of the series $c\ n = 1$, which characterizes the displacement and the ring as a rigid whole, is characteristic. The contact force is written by Eq.

$$p\left(\varphi,\tau\right) = u_0\sum_{i=1}^m k_{0i} + \sum_{n=2}^\infty\sum_{i=1}^m k_{ni}u_n\left(\varphi,\tau\right) \tag{5}$$

where m is the number of shells.

The coefficients k_{0i}, k_{ni} are determined when solving the contact problems of combining a shell with a ring, provided that the stroke is carried out along the line [14]. For a system consisting of coupled spherical (i - 1) and cylindrical shells of finite length: $k_0 = \dfrac{EF}{R^2}\left(1 + \beta_{01} + \beta_{02}\right)$.

In these equations:

$$\beta_{01}=\frac{E_1h_1\sqrt{\dfrac{h_1R}{\sin\theta_0}}}{EF\sqrt[4]{3\left(1-\upsilon_1^2\right)}};$$
$$\beta_{02}=\frac{E_1h_2\sqrt{h_2R}}{EF\sqrt[4]{3\left(1-\upsilon_2^2\right)}};$$
$$\beta_{n1}=\frac{E_1h_1R^3}{2\left(1+\upsilon_1\right)EI}\cdot\frac{\left(1+n\cos\theta_0\right)^2}{n\left(n-1\right)c_n\left(\theta_0\right)};\tag{6}$$
$$\beta_{n2}=\frac{\sqrt[4]{3(1-\upsilon_2^2)}E_2h_2^2R^2}{6\left(1-\upsilon_2^2\right)EI}\sqrt{\frac{h_2}{R}}\frac{f_n}{n\sqrt{n^2-1}}$$

The coefficients $f_n\left(n>1\right)$ characterize the boundary conditions at the other edge of the cylindrical shell. For clamping ($u=\upsilon=0$), free edge ($T_1=s=0$), and free restraint ($T_1=\upsilon=0$), they are as follows:

$$f_{n1}=\left(\exp 4\xi_1b_n-2\exp 2b_n\xi_1\sin 2b_n\xi_1-1\right)\left[\exp 4b_n\xi_1+2\exp 2b_n\xi_1\left(\cos 2b_n\xi_1-2\right)+1\right.$$
$$f_{n2}=\left(\exp 4b_n\xi_1+2\exp 2b_n\xi_1\sin 2b_n\xi_1-1\right)\left[\exp 4b_n\xi_1+2\exp 2b_n\xi_1\left(\cos 2b_n\xi_1+2\right)+1\right.\tag{7}$$
$$f_{n3}=\left(\exp 4b_n\xi_1+2\exp 2b_n\xi_1\sin 2b_n\xi_1-1\right)\left[\exp 4b_n\xi_1+2\exp 2b_n\xi_1\left(\cos 2b_n\xi_1-2\right)+1\right.$$
where
$$b_n=\frac{\sqrt{2}}{2}n\sqrt{n^2-1}\sqrt[4]{\frac{h_2^2}{12R^2\left(1-\upsilon_2^2\right)}}$$

The undisturbed symmetrical form of oscillations is determined from Eq.

$$\ddot{u_0}+s^2+k_0u=0\tag{8}$$

where $s^2=N\left(a^2EF\right)^{-1};k_0=\alpha_0R^3I^{-1};$ with initial conditions: $u_0=0,u_0=\upsilon_0\left(ca\right)^{-1}$ at $\tau=0$ υ_0 is the inward velocity of the ring caused by the pressure pulse $u_0=\dfrac{\upsilon_0}{ca\omega}\sin\omega_0\tau,\omega_0=a^{-2}+k_0E^{-1}$.

The ring tearing out is associated with the emergence of unstable forms of bending vibrations. To determine them, after substituting (4) into (3), we obtain for b_n and d_n, the well-known in the theory of dynamic stability Matier's equation [15]:

$$\ddot{b}_n+p_n\left(\tau\right)b_n=0,$$
where
$$p_n\left(\tau\right)=\left(n^2-1\right)\left(n^2-s^2\sin\omega_0\tau\right)+k_nR^3\left(EI\right)^{-1}=p_{n1}\left(\tau\right)+p_{n2}\left(\tau\right)\tag{9}$$

A negative value of $p_n(\tau)$ defines the range of harmonics for which the motion is unstable. In this case, the corresponding solution to the equation contains $e^{b\tau}$, which leads to a sharp increase in deflection with an increase in τ . In the study of bending vibration forms, the value of s^2 can be considered as a first approximation as a function of u_0 , which is determined by the solution of equation (8)[16]. The obtained dependences allow us to estimate the dynamic stability of the antenna mirror under pulsed edge loading.

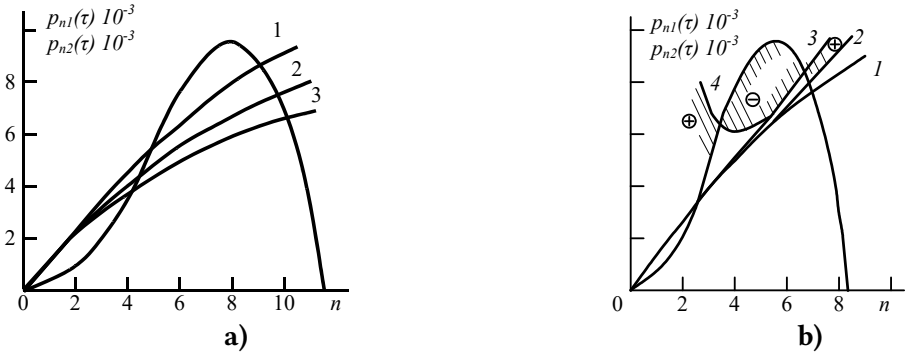

Figure 7: Elastic properties (a, b - shows the dependences characterizing the effect of the spherical coordinate of the sphere edge).

Figures 7 and 8 show some results of the numerical analysis of the dynamic stability of a structure consisting of a cylindrical shell and a spherical mirror.

The following system parameters were used for this purpose:

$$\upsilon_0 = 25m/s, \bar{\delta} = \frac{E_1 h_1 R^3}{2(1+\nu)E_K I_K} = 10^4, I_K = 5\cdot 10^{-4} m^4, R = 1m, E = 7\cdot 10^{10} H/m^2$$

The area of dynamic instability is marked with a minus sign, and the area of stable motion with a plus sign.

In Figure 7 a shows the dependences characterizing the effect of the spherical coordinate of the sphere edge: 1-3 correspond to the spherical coordinate θ_0, which is 45; 50; 55°.

In Figure 7, b - 1 corresponds to the case when the elasticity of the sphere is taken into account; 2 and 3 - the elasticity of an infinite cylindrical shell, respectively, with R/h₂ equal to 250 and 200; 4 limits the dynamic stability region for the case *L/R* = 2 with rigidly clamped edges of the cylindrical shell and the spherical shell with 45° [17].

We study the effect of various boundary conditions on the example of a cylindrical shell.

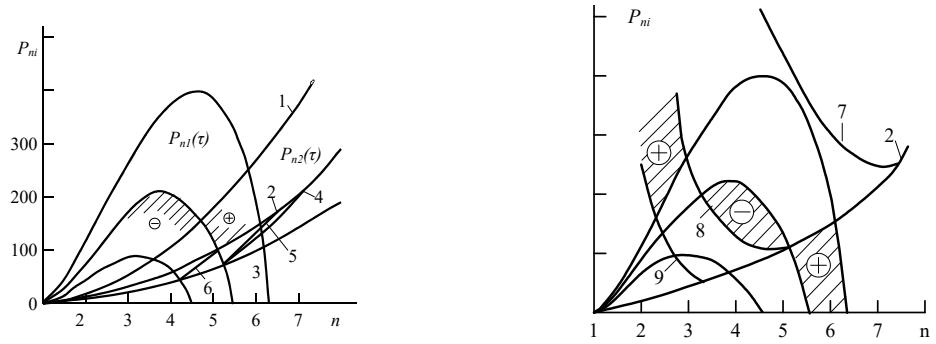

a) **b)**

Figure 8: Areas of instability (a,b - the regions of instability are plotted for an infinite cylindrical shell with parameters R / h_2).

In Figure 8 a, the regions of instability are plotted for an infinite cylindrical shell with parameters R / h_2 equal to 100, 125, and 150 - curves 1-3. For the time $\tau = 0,48 \cdot 10^{-2}$, the regions of dynamic stability determined by the condition $P_{n1}(\tau) > P_{n2}(\tau)$ for $R / h_2 = 100$ are shaded.

Here, for the ratio R / h_2, the regions for the shell with free edges (ring in the middle of the shell) are plotted. Curves 4-6 characterize the shells of dimensionless length at ξ equal to 1; 2; 3 ($\xi = L / 2R$). As can be seen, in this case, R/h has a negligible effect on the appearance of the stability regions.

In Figure 8 b, for $R / h_2 = 125$, the regions of the pinched shells are plotted: 2 - characterizes the stability region for an infinite shell, 7-9 - for pinched shells of dimensionless length when ξ the parameter is equal to 1, 2, or 3, the length of the shell becomes crucial in defining the dynamic stability regions. A shorter shell length leads to a more concentrated stability region, which is associated with a significant increase in stiffness within the system. With a decrease in length, these regions decrease, which is associated with a sharp increase in the stiffness of the system. For the time $\tau = 0,48 \cdot 10^2$ at $\xi = 2$, the corresponding regions are shaded. For $\xi = 1$ in the entire range of numbers $np_{n1}(\tau) > p_{n2}(\tau),$, the motion of the shell at a given impulse is stable. In the calculations, $E = 710 \cdot 10H / m^2, c = 5 \cdot 10^3, \upsilon_0 = 7m / s, I = 2,81 \cdot 10^{-7} m$ (a rectangular ring of unit width with a height of $0,015m$) is assumed, $R = 0,75m,\ \nu = 0,3.$

The previous examples omit the consideration of the shell's inertia, which can be estimated by introducing a specific shell length attached to the ring. This length is selected based on certain key factors and assumptions [18]. It should be noted that when studying the dynamic stability of a shell with a filler, the inertia of the latter is usually also neglected. Using the known solutions for different shells, it is possible to generalize the above solutions to the case of impulse pressure on a ring supporting a system of shells of different classes.

4. Stiffness and stability of shell structures of mirror antennas using simulation modelling

In investigating the dynamic stability of an antenna mirror shaped as a spherical segment and bonded to a ring, various factors and parameters are considered in the design process. To achieve consistency in solutions, the concept of a cylindrical shell attached to the ring, acting as an elastic base, is introduced. This approach allows for the inclusion of design elements such as protection against external influences [19].

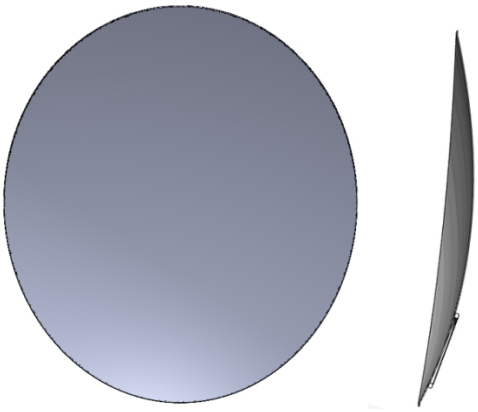

Figure 9: Offset aluminum antenna with a thickness of 2 mm (front view and side view).

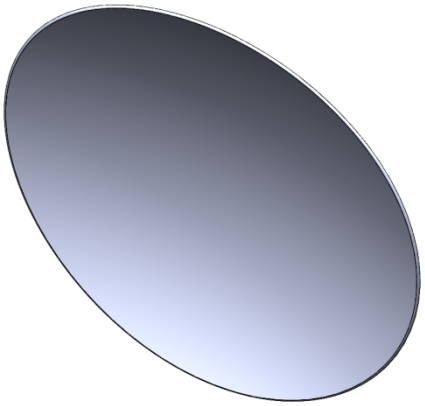

Figure 10: Offset aluminum antenna with a thickness of 2 mm (general view of the antenna, trimetry).

Wind load (Pmax=320 Ra) at a wind speed of 20 m/s

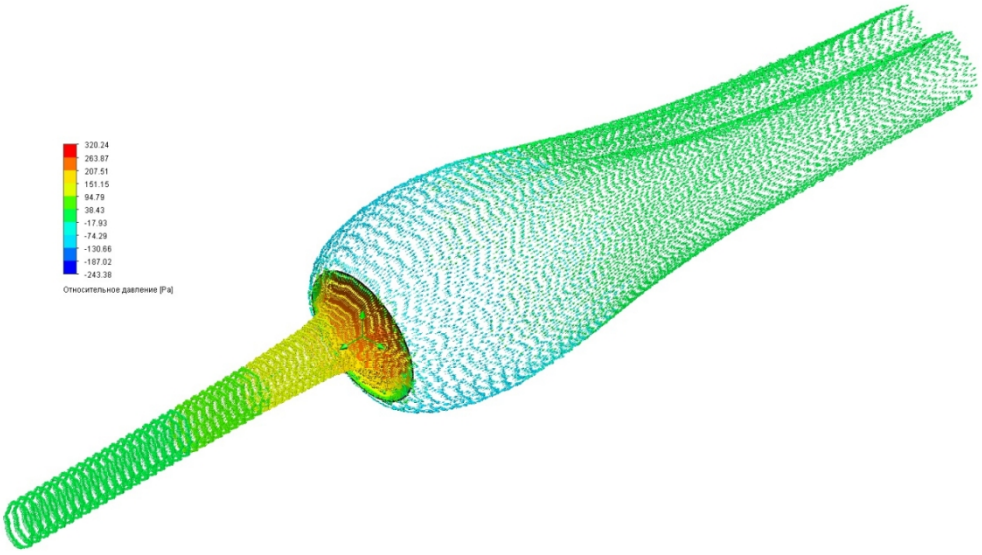

Figure 11: Wind load (Pmax=320 Ra) at a wind speed of 20 m/s.

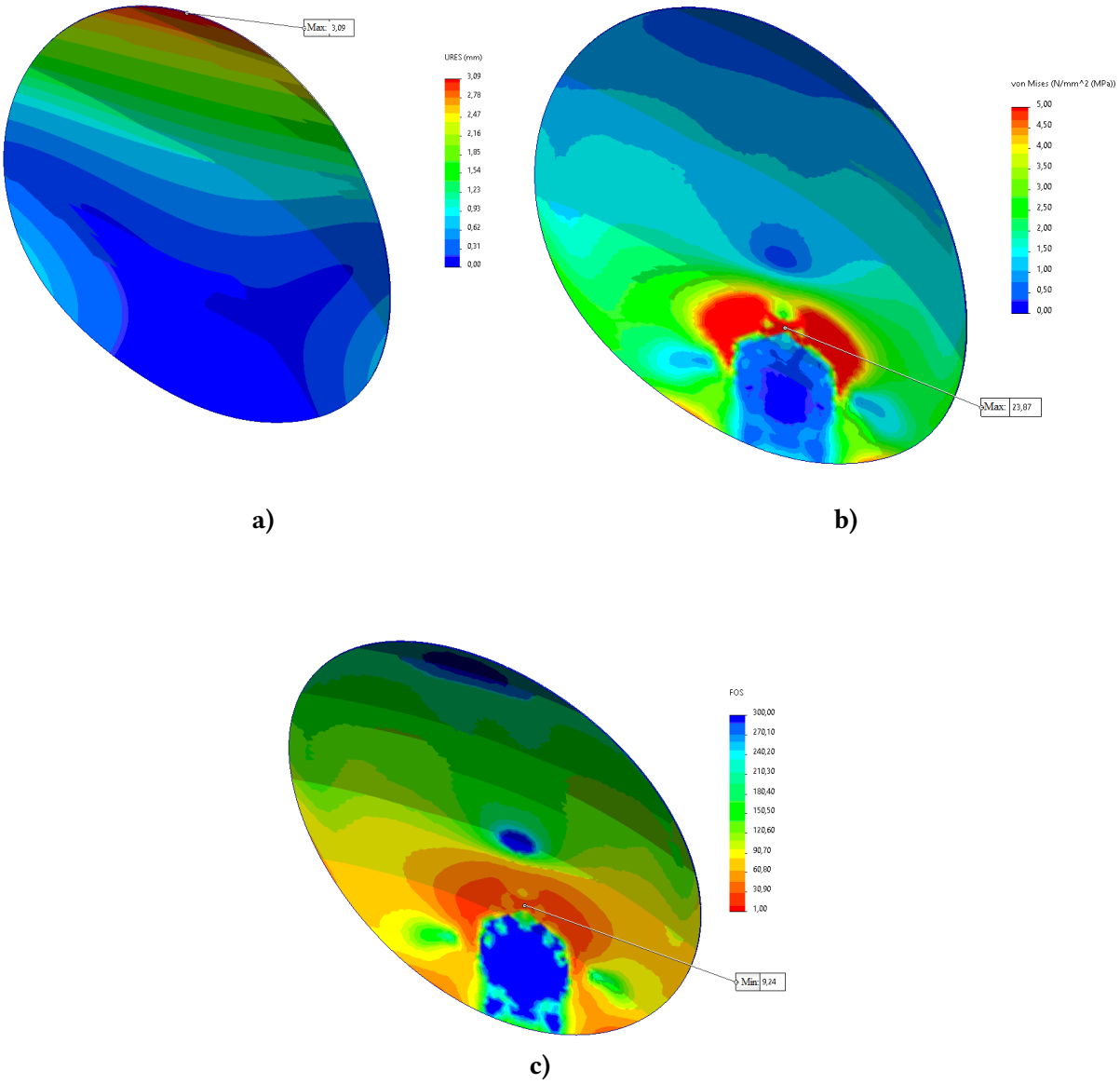

Figure 12: Modelling results (a - displacement epicurve; b - stress epicurve; c - safety factor epicurve).

This study focuses on the efficient application of electric arc spraying technology for the creation of reinforced materials. This technique, which enables the deposition of thin layers of protective material onto various surfaces, holds significant potential across multiple fields, including construction, industry, and telecommunications. The use of electric arc spraying presents opportunities to enhance material strength, provide corrosion resistance, and mitigate other adverse effects experienced by materials exposed to heavy loads, such as wind. Our research examines the specific impact of electric arc spraying on reinforced materials under wind loads, exploring its potential for developing stable and durable structures [20].

The primary stages of electric arc spraying include surface preparation, material preparation, arc generation, spraying, cooling, and fixing. The surface requiring coating must first be meticulously prepared by removing contaminants such as dirt, oil, and rust, and in some cases, it may need grinding or other treatments to enhance the adhesion of the coating. The coating material, typically supplied in the form of wire or powder, is then melted at extremely high temperatures within the electric arc. This process converts the material into molten droplets. These droplets are then sprayed onto the prepped surface using a gas jet, commonly argon or air. Once the molten material contacts the surface, it solidifies quickly, forming a thin, durable layer. After this coating is applied, the surface undergoes a cooling phase, during which the material is fixed securely. Additional post-processes, such as heat treatment or ultrasonic treatment, may be employed to maximize the strength and durability of the coating [21].

Wind loads can significantly impact reinforced materials created using electric arc spraying, particularly for structures exposed to outdoor or elevated environments. These structures may include masts, antennas, towers, and other components used in telecommunications systems, power transmission, or building construction. Wind forces can induce deformations or even structural failures. However, the reinforced material applied through electric arc spraying functions as a protective layer, helping to mitigate the effects of wind loads on the underlying structure. To ensure reliability, calculations must account for potential manufacturing and installation errors, such as improper positioning of antenna components or discrepancies in material properties.

Offset composite antenna with a thickness of 2 mm

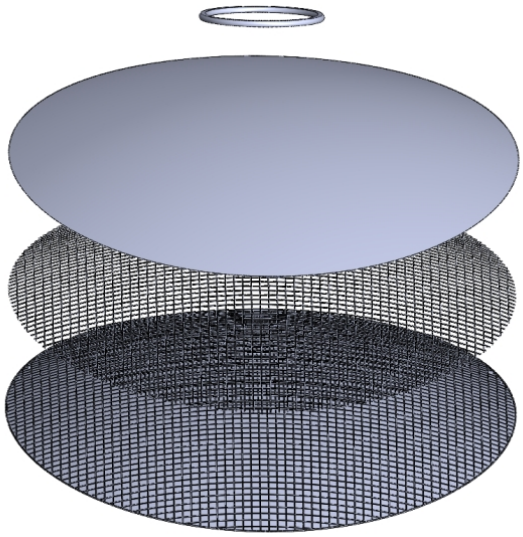

Figure 13: General view of the antenna structure.

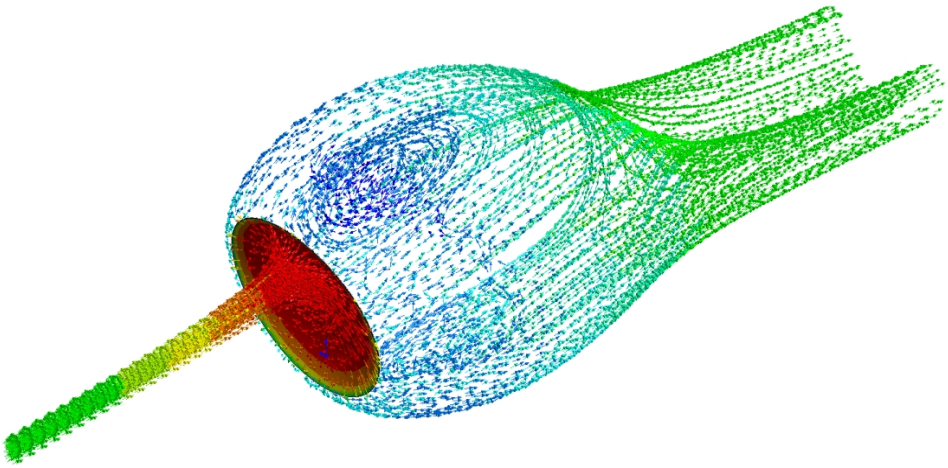

Figure 14: The wind load looks more interesting than in the previous case.

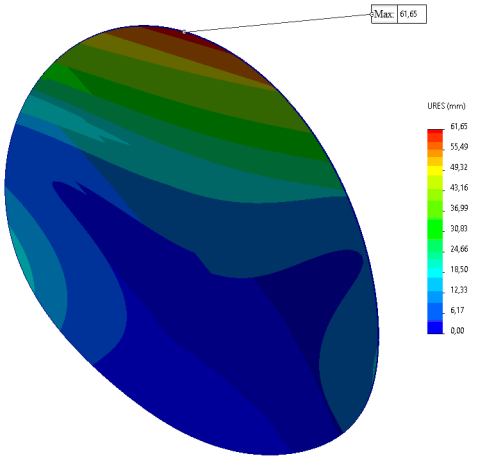

Figure 15: Displacement diagram.

The analysis of the stress-strain state for two different offset antenna designs yielded the following results:

The safety factor for the proposed offset antenna design is 5.7 times lower than that of the basic design. However, it remains above the minimum allowable safety factor of 1.5 for such applications [22].

The normal stresses in the proposed design are 4.5 times higher compared to the basic design, reaching approximately 108 MPa .

The maximum displacements at the top edge of the antenna in the proposed design are 20 times greater than those in the basic design, amounting to roughly 62 mm . Such displacements are significant enough to prevent the antenna from operating normally under the analyzed conditions (e.g., wind loads or environmental factors).

These results highlight the compromises in structural integrity and performance in the proposed design, stressing the importance of optimizing for both stress resistance and displacement limits (wind speed of 20 m/s).

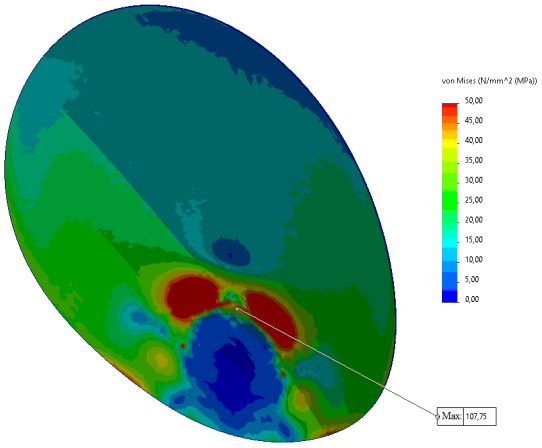

Figure 16: Stress diagram.

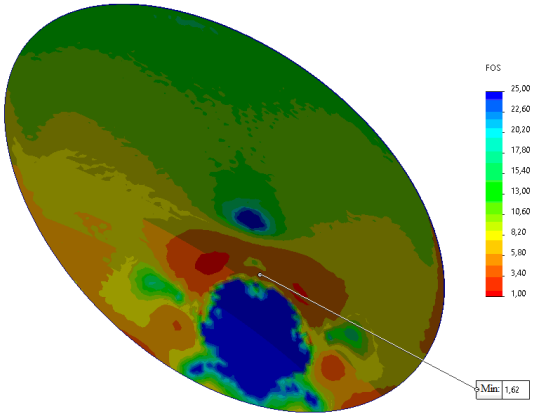

Figure 17: Safety factor diagram.

The obtained results of wind load research can be effectively used for patch antennas with elliptical slits [23] and cyber-physical biosensor systems [24], [25].

Conclusion

In this study, the process of forming reflective shells and determining the positions of mesh elements after deformation was thoroughly examined. The mesh nodes were secured using electric arc spraying. Subsequently, a composite material, such as polystyrene, was applied to create reflective shells.

The outcome of the research was the successful formation of the antenna array shell through electric arc spraying and the application of the composite material. The mirror structure's schematic shows spherical and cylindrical shells joined with a ring, where the shell surrounding the ring acts as an elastic base that restricts movement. To account for the effect of the shell in terms of the ring's motion under pulse pressure, contact forces of interaction were introduced, which were determined by solving the relevant contact problems during mating.

The stiffness-strength characteristics of both solid and reinforced antenna structures were evaluated and illustrated graphically. The stress-strain state of these structures was calculated under the influence of wind forces and gravity.

This research aims to explore the capabilities of offset antennas, highlighting their potential for expanding their application in modern radio engineering systems. As technological advancements continue and communication needs grow, offset antennas are surfacing as innovative and efficient solutions.

The paper also addresses the issue of local stability under load, emphasizing the importance of examining problems related to edge dynamic loads that arise from vibrations in the antenna mirror transmitted from the base.

The study further investigates the dynamic stability of a mirror, formulated as a spherical segment attached to a ring. To maintain consistency, the analysis assumes that a cylindrical shell of finite length is affixed to the ring (a mirror made solely from a spherical shell is considered a special case).

The cylindrical shell's presence is tied to a design aimed at shielding the antenna from external forces, such as airflows. After a pulse is applied, the resulting motion includes both

axisymmetric and bending vibrations, which emerge from unavoidable inconsistencies in pulse distribution.

References

[1] Yavorska M. I., Dubyniak T. S., Manziy O. S., Andreichuk S. K. (2022) Doslidzhennia protsesu ta zadachi, shcho vynykaiut pry utvorenni obolonok metodom elektroduhovoho napylennia [Study of the process and problems arising during the formation of shells by the method of electric arc spraying]. MMMTES (Tern., November 22-23, 2022), pp. 85-87 [in Ukrainian].

[2] The process of shells formation by electric arc spraying method and optimization by the criterion of their geometric shape accuracy / Taras Dubynyak, Roman Dzhydzhora, Oleksandra Manziy, Stanislav Andreichuk // Scientific Journal of TNTU. (- Ternopil : TNTU, 2021). - Vol 104. - No. 4. - P. 24-32.

[3] "Antenna and Wave Propagation" by John D. Kraus and Ronald J. Marhefka (2017, McGraw Hill)

[4] Proakis, J. G. (2006). Digital Signal Processing: Principles, Algorithms, and Applications. Prentice-Hall.

[5] Belytschko, T., Liu, W. K., & Moran, B. (2000). Nonlinear Finite Elements for Continua and Structures. John Wiley & Sons.

[6] Cook, R. D., Malkus, D. S., & Plesha, M. E. (2002). Concepts and Applications of Finite Element Analysis. John Wiley & Sons.

[7] Reddy, J. N. (2014). Introduction to the Finite Element Method. McGraw-Hill.

[8] Zhang, X., & Ainsworth, M. (2010). The Finite Element Method in Electromagnetics. Wiley.

[9] Hughes, T. J. R. (2012). The Finite Element Method: Linear Static and Dynamic Finite Element Analysis. Dover Publications.

[10] Bathe, K. J. (2006). Finite Element Procedures. Prentice-Hall.

[11] Logan, D. L. (2011). A First Course in the Finite Element Method. Cengage Learning.

[12] Zienkiewicz, O. C., Taylor, R. L., & Zhu, J. Z. (2005). The Finite Element Method: Its Basis and Fundamentals. *Elsevier.*

[13] Sadd, M. H. (2009). Elasticity: Theory, Applications, and Numerics. Academic Press.

[14] Ciarlet, P. G. (2002). The Finite Element Method for Elliptic Problems. SIAM.

[15] "Microwave Engineering: Concepts and Fundamentals" by Ahmad Shahid Khan (2014, CRC Press)

[16] "Modern Antenna Design" (3rd Edition) by Thomas A.Milligan (2005, Wiley)

[17] Jin, J. (2014). The Finite Element Method in Electromagnetics. Wiley-IEEE Press

[18] "Practical Antenna Design for Wireless Products" by Henry Lau (2013, Artech House)

[19] Hart E., Hudramovich V., Application of the projection-iterative scheme of the method of local variations to solving stability problems for thin-walled shell structures under localized actions, Strength Mater. 50, no. 6, 852-858, (2018).

[20] Zienkiewicz O., Teylor R., The Finite Element Method for Solid and Structural Mechanics, Elsevier, New York, (2005).

[21] Sinkovsky A. Materials for sawing and welding. Lecture notes for students. Lekts. Specialist. 7.092303 - technol. I statistical analysis of the development and improvement of the reliability of parts of machines and designs, Science and technology, (2008), 128 p.
[22] George, J., Uko, M., Ekpo, S., & Elias, F. (2023). Design of an elliptically-slotted patch antenna for multi-purpose wireless wi-Fi and biosensing applications. In e-Prime - Advances in Electrical Engineering, Electronics and Energy (Vol. 6, p. 100368). https://doi.org/10.1016/j.prime. (2023).100368
[23] Maruschak, P. O., Panin, S. V., Zakiev, I. M., Poltaranin, M. A., Sotnikov, A. L. (2016). Scale levels of damage to the raceway of a spherical roller bearing. In Engineering Failure Analysis (Vol. 59, pp. 69–78). https://doi.org/10.1016/j.engfailanal.2015.11.019
[24] Martsenyuk V., Sverstiuk A., Klos-Witkowska L., Nataliia K., Bagriy-Zayats O., Zubenko I. Numerical analysis of results simulation of cyber-physical biosensor systems (2019) CEUR Workshop Proceedings, 2516, pp. 149 – 164.
[25] Martsenyuk V., Sverstiuk A., Bahrii-Zaiats O., Kłos-Witkowska A. Qualitative and Quantitative Comparative Analysis of Results of Numerical Simulation of Cyber-Physical Biosensor Systems (2022) CEUR Workshop Proceedings, 3309, pp. 134 – 149.